Corrigendum

Corrigendum to: **Crystal structure of human nicotinamide mononucleotide adenylyltransferase in complex with NMN** (FEBS 25964)

[*FEBS Letters 516 (2002) 239–244*]☆

Erik Werner[a], Mathias Ziegler[b], Felicitas Lerner[b], Manfred Schweiger[b], Udo Heinemann[a,c,*]

[a] *Crystallography Group, Max Delbrück Center for Molecular Medicine, Robert-Rössle-Str. 10, D-13092 Berlin, Germany*
[b] *Institute of Chemistry - Biochemistry, Free University of Berlin, Thielallee 63, D-14195 Berlin, Germany*
[c] *Institute of Chemistry - Crystallography, Free University of Berlin, Takustr. 6, D-14195 Berlin, Germany*

First published online 25 June 2002

Structural information on human nicotinamide mononucleotide adenylyltransferase (NMNAT), the enzyme that catalyzes the last step in the biosynthesis of nicotinamide adenine mononucleotide (NAD^+) increased significantly recently. Three groups published crystal structures of hNMNAT, Garavaglia et al. [1] the apoenzyme (PDB code 1kku), Zhou et al. [2] the complex with NAD^+ and deamido-NAD^+ (1kqn/1kqo) and our group [3] the complex with nicotinamide mononucleotide (NMN; 1gry). The two other groups kindly exchanged coordinates with us and made a thorough comparison possible. The polypeptide region from Glu86 to Lys105 of 1gry (the last residue before a missing loop) showed big differences and root mean square difference (rmsd) values up to 10 Å against all other structures. The structural alignment showed that we placed Glu86 into the poorly defined electron density where Garavaglia and Zhou fit Glu86 and Ser87. Refinement of the whole asymmetric unit after rebuilding the residues 86–105 according to the structures of Zhou and Garvaglia indeed revealed that our model was out of register by one residue in this region. After rebuilding the residues in this stretch, the electron density was significantly better explained and most of the *B* factors decreased. Also, the R_{cryst} and R_{free} quality factors decreased by 0.7 and 0.5%, respectively, and the geometry improved. Table 1 summarizes the new refinement statistics. Although no other coordinates than those of residues 86–105 where manually changed, further refinement with REFMAC5 [4] had also some effects on all other coordinates which is reflected in the deposited coordinate file at the Protein Data Bank, where entry 1gry is replaced by the new entry 1gzu. Because of the shift of those 20 residues, three more residues, Leu106, Glu107 and Ala108, could be included into the model. In addition, the secondary structure recognition by the program PROMOTIF [5] changed to a small extent. The site where the shift occurred, residues 85–88, is now recognized as a small helix and causes a renumbering of the helices as shown in Fig. 1a. The oligomerization and protein–protein contacts are not affected since the residues 85–108 are not involved in those. The most significant change is observed at the ligand binding pocket. Glu94 is not involved in substrate binding and Trp92 is not flipped compared to the other ligand binding states (apoenzyme in 1kku, full ligand in 1kqn and 1kqo). Rather, the backbone nitrogen and the sidechain Oγ of Thr95 are in hydrogen-bonding position to O7 of NMN. Trp92 Nε1 may form another hydrogen bond with O2R of NMN and, in addition, forms a 90° hydrophobic contact to the nicotinamide ring that, on the other side, is stacked against Trp169 (Fig. 1b and c). This is now in agreement with the position and orientation of the sidechains in the other structures and with the ligand binding pattern in the structures of Zhou et al. [2]. Further comparison and a model for ligand binding will be published separately.

Table 1
Refinement statistics

R_{cryst}[a] (%)	24.6
R_{free} (%)	28.6
Rmsd bond lengths (Å)	0.017
Rmsd bond angles (°)	1.593
Average *B* factor[b], all atoms (Å^2)	53.6
Average rmsd for main-chain *B*-factors[b] (Å^2)	1.35
Average rmsd for sidechain *B*-factors[b] (Å^2)	4.18

[a] $R_{cryst} = \Sigma|F_{obs} - F_{calc}|/\Sigma|F_{obs}|$.
[b] Calculated with BAVERAGE [4].

References

[1] Garavaglia, S., D'Angelo, I., Emanuelli, M., Carnevali, F., Pierella, F., Magni, G. and Rizzi, M. (2001) J. Biol. Chem. 277, 8524–8530.
[2] Zhou, T., Kurnasov, O., Tomchick, D.R., Binns, D.D., Grishin, N.V., Marquez, V.E., Osterman, A.L. and Zhang, H. (2002) J. Biol. Chem. 277, 13148–13154.
[3] Werner, E., Ziegler, M., Lerner, F., Schweiger, M. and Heinemann, U. (2002) FEBS Lett. 516, 239–244.
[4] Collaborative Computational Project, No. 4 (1994) Acta Crystallogr. Section D50, 760–763.
[5] Hutchinson, E.G. and Thornton, J.M. (1996) Protein Sci. 5, 212–220.

☆SSDI of original article S001-4579(30)20255-6.

*Corresponding author. Fax: (49)-30-9406 2548.
E-mail addresses: ewe@mdc-berlin.de (E. Werner), mziegler@chemie.fu-berlin.de (M. Ziegler), heinemann@mdc-berlin.de (U. Heinemann).

PII: S0014-5793(02)02984-8

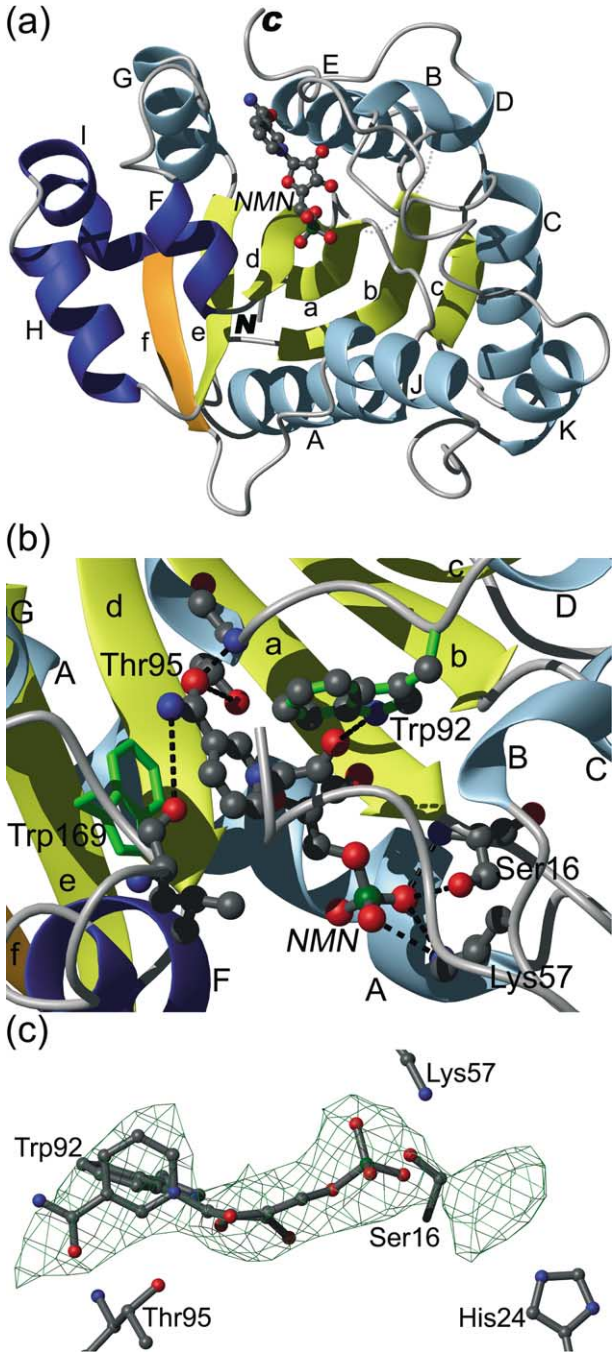

Fig. 1. a: Ribbon model of human NMNAT in complex with NMN. Strands are in yellow/orange, helices in light and dark blue; atom colors: C, gray; N, blue; O, red; P, green. b: NMN binding site of hNMNAT (chain A). Hydrogen bonds between protein residues and the ligand are shown as dotted lines, color code as above. The C-terminus is seen at the center of the image. c: F_o-F_c difference electron density around the ligand (chain A). Calculated after refinement of the final model without the ligand, contoured with 2σ. Ball-and-stick representations of the ligand and adjacent amino acid sidechains are shown.